Application of Self-Organizing-Maps Technique in Downscaling GCMs Climate Change Projections for Same, Tanzania

S.D. Tumbo[a], E. Mpeta[b], B.P. Mbillinyi[a], F.C. Kahimba[a*], H.F. Mahoo[a], and M. Tadross[c]

[a] Department of Agricultural Engineering and Land Planning, Sokoine University of Agriculture, P. O. Box 3003 Morogoro, TANZANIA.
[b] Tanzania Meteorological Agency (TMA), P. O. Box 3056, Dar es Salaam, TANZANIA.
[c] Department of Environmental & Geographical Science, University of Cape Town, Rondebosch 7701, SOUTH AFRICA.

ABSTRACT

High resolution surface climate variables are required for end-users in climate change impact studies; however, information provided by Global Climate Models (GCMs) has a coarser resolution. Downscaling techniques such as that developed at the University of Cape Town, which is based on Self-Organizing Maps (SOMs) technique, can be used to downscale the coarse-scale GCM climate change projections into finer spatial resolutions; but that must be combined with verification. The SOM downscaling technique was employed to project rainfall and temperature changes for 2046-2065 and 2080-2100 periods for Same, Tanzania. This model was initially verified using downscaled NCEP reanalysis and observed climate data set between 1979 and 2004, and between NCEP reanalysis and GCM controls (1979 - 2000). After verification, the model was then used to downscale climate change projections of four GCMs for 2046-2065 (*future-A*) and 2080-2100 (*future-B*) periods. These projections were then used to compute changes in the climate variables by comparing *future-A* and *B* to the control period (1961-2000). Verification results indicated that the NCEP downscaled climate data compared well with the observed data. Also, comparison between NCEP downscaled and GCM downscaled showed that all the four GCM models (CGCM, CNRM, IPSL, and ECHAM) compared well with the NCEP downscaled temperature and rainfall data. Future projections (2046-2065) indicated 56 mm and 42 mm increase in seasonal total rainfall amounts for March-April-May (MAM) and October-November-December (OND) (23% and 26% increase), respectively; and a temperature increase of about 2°C for both seasons. Furthermore, it was found that during MAM there will be a decrease in dry spells by 2 days, and an increase in seasonal length by 8 days, while for OND, there will be also 2 days decrease in dry spells, and 40 days increase in the seasonal length. The results for *future-B* shows a 4°C rise in temperature, and 46.5% and 35.8% increase in rainfall for MAM and OND, respectively. The results imply a better climatic future for the area because of the increase in the amount of rainfall and decrease in dry spells. However, it is suggested that further investigations are required to see if the projected changes will have real positive effects in agricultural production and also identify better agronomic practices that will take advantage of the opportunities.

Keywords: climate change, downscaling, GCMs, Self Organizing Maps, NCEP, Tanzania

1. Introduction

Agriculture is the leading sector of the economy of Tanzania. It accounts for over half of the Gross Domestic Product (GDP), provides 85% of export earnings, and employs over 80% of the work force (URT 2001). Unfortunately, as in other African countries, the sector is highly vulnerable to climate change and variability because of its over-dependence in rainfall. According to World Bank (2002), only 3.3% of the cropland was irrigated in Tanzania as of 1999. The remaining area depended on rainfed agriculture. Hence, any attempts to improve agriculture must therefore tackle the problems associated with climate change and its variability.

*Corresponding author: *E-mail address* fredkahimba@.suanet.ac.tz; kahimbafcs@yahoo.com *(F.C. Kahimba)*

In order to capture the climate change issues relevant for agricultural production, location-based assessments are needed to complement the broad impact assessments such as those provided by Global Climate Models (GCMs) (Feenstra et al., 1997). GCMs represent physical processes in the atmosphere, ocean, cryosphere, and land surface. They are widely known to be the most advanced tools currently available for simulating the response of the global climate system to increasing greenhouse gas concentrations (Kistler et al., 2001; Wilby et al., 2004). The GCMs are capable of simulating the general circulation as well as inter-annual oscillations such as El Nino - Southern oscillation (ENSO), and forecasting climate trends decades or hundred of years in advance. Although simpler models have also been used to provide globally- or regionally-averaged estimates of the climate response, only GCMs, possibly in conjunction with nested regional models, have the potential to provide geographically and physically consistent estimates of regional climate change which are required in impact studies (Houghton et al., 2001). GCMs depict the climate using a three-dimensional grid over the globe typically having a horizontal resolution of between 250 and 600 km, 10 to 20 vertical layers in the atmosphere, and sometimes as many as 30 layers in the oceans (Houghton et al., 2001). Their resolution is thus quite coarse relative to the scale of exposure units in most impact studies.

Downscaling techniques are commonly used to address the scale mismatch between coarse resolution GCM outputs and the regional or local scales (Kistler et al., 2001; Wilby et al., 2004; Spak et al., 2007). The techniques are used to provide insights at scales essential to stakeholders and policy makers to better assist users to assess the potential impacts of climate change and plan to adapt. Several methodologies to downscaling are available. Generally, the methodologies fall into two broad categories (Corell, 2007). The first category is called dynamic downscaling, and its basic approach is to nest a finer-scale grid within a GCM over an area of interest. Despite some advantages of the dynamic downscaling, the methodology requires supercomputer systems and there are too few supercomputer systems available to perform such mesoscale simulations to fully assess the local/regional impacts and consequences of climate change (Corell, 2007). As supercomputer capabilities and availability increases, dynamic downscaling will become more widely accessible.

The second category, statistical or empirical downscaling (SD), is a fully developed and widely used technique for exploring the regional and local-scale response to global climate change as simulated by comparatively low-resolution GCMs. The technique involves developing quantitative relationship between large-scale climate variables ("predictors") and local surface variables ("predictands"). As long as significant statistical relationships occur, empirical downscaling can yield regional information for any desired weather variable such as precipitation and temperature. As noted in the third assessment report (TAR) of the intergovernmental panel on climate change (IPCC, 2001), SD has a wide appeal because it is computationally inexpensive and can easily be applied to a large number of climate simulations. This makes it particularly attractive to the impacts community and especially to developing countries. The TAR highlights the extensive and diverse list of SD techniques that have been applied to climate downscaling (IPCC, 2001: Chapter 10, Appendix A). The techniques can generally be grouped into three categories: transfer function, weather typing, and weather generators. The optimal choices of model type and strategy depend on the problem; hence no general advice can be given (Corell, 2007). The implementation of SD techniques, however, requires a number of assumptions concerning the input data and subjective decisions on the choice of statistical parameters. An important assumption for the validity of SD is that of stationarity of the downscaling function, i.e. the relationship between the predictors and predictand remains valid for periods outside the fitting period (Hewitson and Crane, 2006).

This paper presents an evaluation of downscaled climate projections for Same, located in the North-Eastern Tanzania near Mt. Kilimanjaro. The study of climate change in Tanzania, including Same, is also reported by Matari et al. (2008). This was a country level study and which showed that mean annual temperature in the North-Eastern areas including Same will increase by 1.7^{o}C by 2100 in comparison to 1961-1990 baseline. Precipitation over the whole country is expected to increase by 10%, and for North-Eastern rainfall is expected to increase by 18% for the period of March to May, period when this area receives most of its reliable rainfall. The study by Matari et al. (2008) used MAGICC/SCENGEN

software to do the downscaling and used five GCM models including ECH3 and UK HIGH considering doubling of carbon dioxide ($2xCO_2$).

This study aimed at investigating how the climate change will impact Same area given the current challenges that farmers are facing by looking in detail into rainfall parameters that affect crop growth such as dry spells, length of growing season, and rainfall amounts. The study used self-organizing map downscaling (SOM) technique to downscale climate data from four GCMs models (CGCM, CNRM, IPSL and ECHAM), forced by the SRES A2 emissions scenario. The A2 scenario is preferred in impacts and adaptation studies because it assumes that if one can adapt to a larger climate change, then the smaller climate changes of the lower end scenarios can also be adapted too (IPCC, 2000; NARCCAP, 2008).

The study investigated how well the GCM models predict the current situation of rainfall and temperature as well as how well they quantify the future projections as defined by IPCCC. Specifically, the study (i) evaluated the SOM model for downscaling temperature and rainfall projections for Same meteorological station; (ii) evaluated the GCMs models ability to simulate the current temperature and rainfall for Same for the control period (1979 to 2000); and (iii) projected changes in rainfall and temperature for *future-A* (2046 - 2065) and *future-B* (2081 - 2100).

2. Materials and Methods

2.1 The study location

The Same meteorological station (Figure 1), located in the north eastern part of Tanzania, was selected for testing the downscaling method. Same district lies on the foothills of the Western Pare Mountains, which are part of the Eastern Arc Mountains. The area is semi-arid with highly variable and unreliable rainfall, with farmers strongly attached to growing maize as their main food crop. Rainfall is bimodal with lowlands receiving less than 500 mm per year and crop failure due to water deficit is common (Enfors and Gordon, 2007).This location was purposely selected because it is a study location for a project under a programme on "Climate Change Adaptation for Agriculture" funded by the Department of Foreign Affairs and International Development (DFID), UK and International Department for Relations and Cooperation (IDRC), Canada.

Figure 1.

Rainfall on the area is highly variable both annually and seasonally. The annual precipitation (1957-2004) averaged at 562 mm, with a standard deviation (SD) of 193 mm (Enfors and Gordon, 2007). The area has two distinct rain seasons, the long (*Masika*) and the short (*Vuli*) rains. For the Masika season the average annual precipitation is 251 mm (SD 119 mm), and for Vuli seasons it is 194 mm (SD 128 mm). There is increased frequency of dry-spells longer than 21 days for Masika seasons. Between 1957 and 1980, 42% of the Masika seasons were affected by dry-spells longer than 21 days, compared to 79% between 1981 and 2004. This represents almost a doubling of the frequency. The long dry-spells often occur relatively later in the season (around day of the year 50-70).

2.2 Downscaling

This study used Self-organizing maps (SOMs) empirical downscaling technique (Hewitson & Crane, 2006). The technique was used to downscale daily rainfall and temperature data for Same meteorological station. The SOMs technique was used to characterize the state of the atmosphere of that location on the basis of NCEP 6-hourly reanalysis data from 1979 to 2004, and using surface and 700-hPa *u* and *v* wind vectors, specific and relative humidity, and surface temperature. Each unique atmospheric state was associated with observed temperature and rainfall density functions (PDF). With such associations, models based on SOM technique were then developed for each climate variable (rainfall, minimum temperature and maximum temperature). Using these models, the future climate conditions (2046 to 2065 and 2081 to 2100) were derived from four global climate models (GCMs): CGCM, CNRM, IPSL, and ECHAM.

Table 1.

In each case, the GCM data were mapped to the NCEP SOMs and temperature values (minimum/maximum) were drawn at random from the associated temperatures PDF. The same procedure was employed to obtain downscaled values for rainfall. More details on the methodology are given by Hewitson and Crane (2006).

2.3 Statistical analysis

2.3.1 Analysis of temperature data

Observed daily maximum and minimum temperatures and downscaled daily NCEP reanalysis maximum and minimum temperatures were compared by running simple linear regression to obtain coefficient of determination (R^2). The same was done to compare NCEP reanalysis and GCMs.

2.3.2 Analysis of rainfall data

Rainfall analysis was divided into the two rainfall seasons (March-April-May and October-November-December, abbreviated as MAM and OND, respectively). Statistical parameters commonly used to characterize rainfall season were computed for each season, which are:

(i) the number of events greater or equal to 2 mm rainfall (counts)
(ii) the number of events greater or equal to 10 mm rainfall (counts)
(iii) rainfall amount (mm)
(iv) maximum dry spells (days)
(v) start of the season (day of the year)
(vi) end of the season (day of the year)
(vii) length of the season (days)

Comparison of the means of these parameters between observed and NCEP reanalysis was then done to obtain statistical differences at $p<0.05$ and $p<0.01$.

2.3.3 Analysis of future changes

To quantify the magnitude of rainfall changes between control period (1961 to 2000), and 2046-2065 (*future-A*) and 2081-2100 (*future-B*) periods, the same seven rainfall parameters (> 2 mm rains, > 10 mm rains, rainfall amount, maximum dry spells, start of the season, end of the season, and seasonal length), were computed for each period. The difference between the mean values for the control period and *future-A* and *future-B* were also computed to quantify the magnitude of change and statistical difference of the determined means.

For temperature analysis, temporal variations of maximum temperature changes for *future-A* were plotted for different GCMs. In addition, the annual changes in minimum and maximum temperatures for the two future periods were also determined.

3. Results and Discussions

3.1 Verifications of the SOM-based downscaling technique

This section provides verification results of the SOM-based downscaling technique for daily minimum temperature, daily maximum temperature, daily rainfall, and NCEP reanalysis. The predicted maximum and minimum temperatures based on NCEP reanalysis as predictors were compared against the observed maximum and minimum temperature values using dataset of the period between 1979 and 2004. Figure 2 presents scatter plots between observed maximum and minimum daily temperatures, and SOM-based and NCEP reanalysis predicted values.

Figure 2.

The predicted maximum and minimum air temperatures based on NCEP reanalysis compared well with the observed values with R^2 values of 0.94 and 0.95 for the maximum and minimum air temperatures, respectively. With regard to rainfall verification, Table 2 presents the comparison between derived seasonal rainfall parameters from the predicted daily rainfall using NCEP reanalysis and observed rainfall for the March-April-May (MAM). The same comparison for the October-November-December (OND) season is presented in Table 3.

Table 2.

Table 2 shows that there was no significant difference ($\alpha = 0.05$) for most of the rainfall parameters with exception of the minimum rainfall. The SOM-based technique significantly under-predicted the minimum rainfall obtained in the period between 1979 and 2004 with observed value being 118.0 mm and predicted value being 28.04. Even the seasonal rainfall, minimum 2 mm and 10 mm rainfall events were under-predicted but were statistically not significant. However, since one of the observed climate change behavior is the increase of extreme events, therefore inability of models to pick some of these extreme behavior might have an impact on the overall assessment of the ability of these models in climate change projection.

Table 3.

During OND the mean rainfall parameter values agreed very well ($\alpha = 0.05$) between observed and predicted rainfall (Table 3). However, the SOM technique significantly under-predicted the maximum and minimum seasonal rainfall, and the 10 mm rain events. Also, with no statistical significance under-predicted the maximum number of the 2 mm rain events (38 vs. 28) but over-predicted the minimum events (2 vs. 6). Further observations show that seasonal rainfall was also under-predicted, and the observed data had more variability compared to rainfall derived using NCEP reanalysis and SOM technique. This again has similar implications as has been indicated in the MAM season with regard to extreme events; however, the OND has more disagreement with predicted conditions compared to MAM. The possible reason might be that MAM has more reliable and stable rainfall compared to OND as it has also been pointed out by Enfors and Gordon (2007).

3.2 Evaluation of the GCMs-based predictions for daily temperature and rainfall

The SOM-based model for predicting daily minimum and maximum temperature and rainfall verified in 3.1 was used to downscale the same daily parameters using NCEP reanalysis between years 1979 and 2000, with the aim of evaluating GCMs predictions. Daily rainfall and temperature data were downscaled using SOM-based models using the four GCM controls between years 1979 and 2000, then compared with NCEP reanalysis to determine how well the GCMs explain the current weather conditions. Figure 3 presents comparison of the downscaled maximum temperature predictions based on the GCM models. The results show good maximum temperature prediction by all the four models with R^2 values ranging between 0.75 and 0.89; however, there was a slight tendency of the models to over-predict temperature values between 28^{o}C and 30^{o}C and under-predict temperatures beyond that window. The minimum temperature predictions also followed a similar trend.

Figure 3.

Comparison between derived parameters from downscaled daily rainfall based on NCEP reanalysis and GCMs controls for the period from 1979 to 2000 is presented in Table 4 for the MAM season. The same comparison for the OND season is presented in Table 5. The seven rainfall parameters used for the comparison were the seasonal rainfall amounts, >2 mm rains, >10 mm rains, dry spell runs, seasonal start dates, end dates, and the seasonal length.

Table 4.

During the MAM season the CGCM, ECHAM, and CNRM performed better than IPSL since all the seven parameters had no significant difference ($\alpha = 0.05$) with the NCEP reanalysis parameters (Table 4). The

IPSL had significantly longer end dates (175.8 vs. 149.1 days) and seasonal length (77.6 vs. 101.0 days). Also, the seasonal total rainfall was much lower for ECHAM compared to NCEP reanalysis (168.2 vs. 208.1 mm) even though the difference was not statistically significant. However, this under-prediction by ECHAM might be significant because already the mean amount predicted by the SOM technique using NCEP reanalysis was lower (Section 3.1).

Table 5.

During OND season the CGCM, IPSL, and ECHAM corresponded well with the NCEP reanalysis (Table 5) with all the seven parameters having no significant difference ($\alpha = 0.05$). The CNRM model had the least performance during OND with four out of seven parameters being significantly different from the NCEP reanalysis (Table 5). However, it predicted well the start dates, end dates, and seasonal length. ECHAM and CNRM predicted much better the end dates and length of the season, respectively, compared to other models.

In general, all the four GCMs (IPSL, CGCM, CNRM, and ECHAM) downscaled data corresponded well with the NCEP reanalysis downscaled data with some slight weaknesses in the two models, which are IPSL showing weakness during MAM and CNRM showing weakness during OND. However, the two models are very strong in predicting the other parameters, which were seen not to be statistically different. Table 6 provides guidance if one has to choose priorities on GCM models and their abilities in predicting specific parameters. Table 6 indicates that in most cases a combination of GCM models provide better prediction of a given variable rather than one GCM model for all or for one specific parameter.

Table 6.

3.3 Projected rainfall changes

3.3.1 Future-A (2046 – 2065)

This section present results of the SOM-downscaling of the GCMs simulated data for future climate for the period from 2046 to 2065, referred here as *future-A*. The values were compared against their corresponding GCM controls or baseline (i.e. 1961 to 2000) in order to determine the change in the rainfall patterns. Results of the *future-A* projections for the MAM season are presented in Table 7. The corresponding *future-A* projections for the OND season are presented in Table 8.

Table 7.

The projections based on the downscaled GCM data for MAM season shows an increase in seasonal rainfall amounts, decrease in dry spells, earlier start dates, later end dates, and longer seasonal lengths during all the two seasons (Table 7). The CGCM, IPSL, and CNRM models indicated a significant increase in rainfall amounts (69.4, 61.0, and 49.6 mm, respectively). The same models showed a significant increase in the >2 mm rainfall events where as a significant increase in >10 mm rainfall events is shown by CGCM and IPSL models only. The four models had an average of about 56 mm increase in rainfall (22.9% increase), 2-days less dry-spells, 2- to 3-days earlier start dates, 5-days later end dates, and 8-days longer seasons.

Table 8.

During OND a trend very similar to that of MAM was observed (Table 8). Rainfall is expected to increase by 43.5 mm, which is a 26.2% increase. On average, the start dates were 5 days earlier; end dates 35 days later; seasonal length 40 days more, and dry spells decreased by 2 days. The most significant changes during OND were recorded by the CGCM and ECHAM_5 models, followed by IPSL and CNRM models. The CGCM showed significant increase on the end dates and seasonal length, CNRM and ECHAM showed a significant increase in the >2 mm and >10 mm rainfall events; but also ECHAM showed a significant increase in the rainfall amount compared to its baseline. The increase in the seasonal end date has more significance because of the dry spells that exist in mid January and February, which separate the two seasons, i.e. *vuli* and *masika*. There is likeliness of the two seasons to merge at that time if the

projected climate changes will not be reversed. Furthermore, the significant increase in the >2 mm and >10 mm events as shown by some GCM models signify that extreme events will increase. Also, the non-significant decrease in dry spell indicates that the research and development on techniques for soil moisture conservation should continue.

3.3.2 Future-B (2081 – 2100)

The *future-B* rainfall projections are presented in Tables 9 and 10 for the MAM and OND seasons, respectively. On average, the GCM models predicted much more significant changes on *future-B* compared to the *future-A* period. During the MAM there was a significant increase in rainfall amounts as indicated by the CGCM (153 mm), IPSL (104.2 mm), CNRM (101.6 mm), and ECHAM (93.8 mm), with an average of 113 mm (46.5% increase). These models also predicted that on average there will be 3 days decrease in dry spells, 6 days earlier start dates, 10 days later end dates, and 16 days longer seasons (Table 9).

Table 9.

During OND the CGCM and IPSL had 5 out of 7 parameters that were significantly different ($\alpha = 0.05$). The CNRM had 4 out of 9 while ECHAM had 3 out of 7 significantly different parameters. The increase in rainfall is estimated to be 58 mm (35.8%-increase) compared to observed rainfall between 1961 and 2000. This implies that more changes will occur during OND than during MAM.

Table 10.

The rainfall projection results indicate that GCM models that corresponded well with the NCEP reanalysis during control period also predicted significant increases in the rainfall parameters of both *future-A* and *future-B*. A greater increase in the OND seasonal length (21-60 days on *future-A*, and 11-80 days on *future-B*) suggests that the OND may join with the MAM to form one longer rainy season (*unimodal*) with a few to no dry spells in between. The projected decrease in dry-spells and increase in the rainfall amounts indicates that the rainfall distribution within specific season will be more stable and crops needing more rains could be grown in those areas. However, increased rainfall amounts also could increase nutrient leaching resulting in more fertilizer requirements (Watson et al., 1998). All models predict fairly stable seasonal start dates, but highly variable and increased end dates.

3.4 Projected temperature changes

Figure 4 presents the projection of annual temporal maximum temperature changes by different GCM models for the *future-A* (2046 to 2065). Results of projected maximum temperature for the *future-A* and *future-B* are presented in Table 9. The projected minimum temperatures are presented in Table 10.

The CCCMA model showed that as the year progresses, on average, the temperature change increases moderately. The greater temperature change occurs around early October. The CNRM model showed a constant increase in temperature from January to July; the greater change in temperature occurring in September/October. The IPSL model shows on average the temperature will increase. The ECHAM model indicates that the temperature increase from January to May will be lower compared to temperature increase from June to December, with small minor dipping around October. In summary, three models (CCCMA, CNRM and ECHAM) indicate that second half of the year will have a greater temperature change compared to the first half. The time of occurrence coincide with the start of the *vuli* season.

Figure 4.

In Table 9, the GCM models indicated 2 and 4 degrees increase in the annual maximum temperatures during the *future-A* and *future-B*, respectively. The annual minimum temperature was also projected to increase by 2.1 and 4.3 degrees in *future-A* and *future-B*, respectively (Table 10). All the GCM models had fairly equal maximum temperature predictions with mean maximum temperatures ranging between 30.6°C and 31.4°C during *future-A*, and 32.3°C and 33.7°C during *future-B*. Models that indicated the

largest maximum temperature change during *future-A* were IPSL (2.3°C), and CNRM (2.2°C). For the *future-B*, the models were IPSL (4.5°C), CNRM (4.4°C), and ECHAM_5 (4.1°C).

Table 11.

Table 12.

For the minimum temperature projections, again the models had fairly equal predictions with annual minimum temperatures ranging between 19.5°C and 20.3°C for *future-A*, and between 21.1°C and 22.7°C during *future-B*. The largest changes in minimum temperatures during *future-A* were recorded by IPSL (2.4°C) CNRM (2.3°C), and CGCM (2.2°C). During *future-B* the largest minimum temperature changes were recorded by IPSL (4.9°C), CNRM (4.7°C), ECHAM_5 (4.5°C), and CGCM (3.9°C). Results obtained concur with IPCC fourth assessment report (FAR) (Meehl et al., 2007), which shows that temperature in the area will increase by 1.5 to 2.0 degrees for *future-A* and by 3.0 to 4.0 degrees for *future-B* based on SRES A2 scenario. The FAR also indicates an increase of about 0.3 mm/day for precipitation for the period 2080 to 2099 based on SRES A1B scenario. In this study, the increase is estimated at 0.46 mm/day based on SRES A2 scenario, which correspond well with the FAR. This value was obtained by summing projected mean increase for MAM (113 mm) and for OND (58 mm) and dividing by 365 days. Therefore, crop maturity time will likely decrease because of temperature increase; however, an increase in temperature may also be associated with increased risk of crop damage from pests and diseases (Watson et al., 1998).

4. Conclusions

The validity of using SOM-based downscaling technique was investigated together with evaluation of GCM models (CGCM, CRNM, ISPL and ECHAM) for projecting climate change in Same, a location in the North-Eastern Tanzania. The SOM-based downscaling predicted well the maximum and minimum temperatures based on NCEP reanalysis data (R^2 = 0.94-0.96). Also, the mean and maximum rainfall based on NCEP reanalysis data compared well with the observed values; however, the minimum rainfall was underestimated (28.0 vs. 118.0 mm) during MAM and was overestimated (46.6 vs. 17.5 mm) during OND. The SOM-based downscaling using GCM control data compared well with the NCEP reanalysis data for temperature and rainfall during both the *masika* (MAM) and *vuli* (OND) seasons, indicating that the SOM technique and GCMs can be used for climate change projections.

Future rainfall projections by the GCM models indicated an increase in rainfall amounts, decrease in dry spells, earlier start dates, later end dates, and longer seasonal lengths, during all the two seasons. During MAM season of *future-A* (2046-2065) the models indicated an average of 56 mm increase (26.2% increase) in rainfall, 2 days less dry-spells, 3 days earlier start dates, 5 days later end dates, and 8 days longer seasons. The GCM models that corresponded well with the NCEP reanalysis during control period also predicted significant increases in the rainfall parameters of both *future-A* and *future-B*. A greater increase in the seasonal length during OND (40 days on *future-A*, and 62 days on *future-B*) gives an indication of the possibility for the OND and MAM seasons (*bimodal*) to form one longer rainy season (*unimodal*).

The maximum and minimum air temperatures are projected to increase by 2.0°C and 2.1°C, respectively, during *future-A*, and by 4.0°C and 4.3°C, respectively, during *future-B*. The projected increase in rainfall amounts and the maximum and minimum air temperatures will favor crops that require more rains. Therefore, more detailed studies are required to investigate the suitability of existing agronomic practices and alternative options for future climates. This can be achieved by employing crop simulation models such as APSIM, PARCHED-THIRST, and DSSAT so as to simulate daily events and how different crops and crop varieties respond to future climates.

Acknowledgements

This publication was supported by the Climate Change Adaptation in Africa (CCAA) program, a joint initiative of Canada's International Development Research Centre (IDRC) and the United Kingdom's Department for International Development (DFID). Also, thanks to the Department of Environmental & Geographical Science, University of Cape Town, Rondebosch, for allowing the use of the Self-Organizing Maps Downscaling (SOMD) technique. The views expressed are those of the authors and do not necessarily represent those of DFID, IDRC, or the Department of Environmental & Geographical Science, University of Cape Town.

References

Enfors, E.I. and Gordon, L.J., 2007. Analyzing resilience in dryland agro-ecosystems: A case study of the Makanya catchment in Tanzania over the past 50 years. Land Degradation and Development. 18: 680-696.

Feenstra, J.F., Burton, I., Smith, J.B. and Tol, R.S.J. (Eds.)., 1998. Handbook on Methods for Climate Change Impact Assessment and Adaptation Strategies. Nairobi and Amsterdam: UNEP and Institute for Environmental Studies/Vrije Universiteit.

Gutierrez, J.M., Cano, R., Cofino, A.S. and Sordo, C., 2005. Analysis and downscaling multi-model seasonal forecasts in Peru using self-organizing maps. Tellus 57A: 435-447.

Hewitson, B.C. and Crane, R.G., 1996. Climate downscaling: techniques and application. Climate Research 7: 85-95.

Hewitson, B.C. and Crane, R.G., 2006. Consensus between GCM climate change projections with empirical downscaling: Precipitation downscaling over South Africa. International Journal of Climatology 26: 1315–1337.

Houghton, J.J., Ding, Y., Griggs, D.J., Noguer, M., van der Linden, P.J., Dai, X., Maskell, K. and Johnson, C.A. (eds)., 2001. What is GCM? IPCC (Intergovernmental Panel on Climate Change). IPCC Working Group I, Cambridge University Press: Cambridge, p. 881.

Kistler, R., Kalnay, E., Collins, W., Saha, S., White, G., Woollen, J., Chelliah, M., Ebisuzaki, W., Kanamitsu, M., Kousky, V., van den Dool, H., Jenne, R. and Fiorino, M., 2001. The NCEP–NCAR 50-year reanalysis: Monthly means CD-ROM and documentation. Bulletin of the American Meteorological Society 82(2): 247-268.

Matari, E.E., Chang'a, L.B., Chikojo, G.E. and Hyera, T., 2008. Climate change scenario development for second national communication – Tanzania. Tanzania Meteorological Agency Research Journal. 1(1): 8 - 17.

Meehl, G.A., Stocker, T.F., Collins, W.D., Friedlingstein, P., Gaye, A.T., Gregory, J.M., Kitoh, A., Knutti, R., Murphy, J.M., Noda, A., Raper, S.C.B., Watterson, I.G., Weaver, A.J. and Zhao, Z.C., 2007. Global Climate Projections. In: Climate Change 2007: The Physical Science Basis. Contribution of Working Group I to the Fourth Assessment Report of the Intergovernmental Panel on Climate Change [Solomon, S., D. Qin, M. Manning, Z. Chen, M. Marquis, K.B. Averyt, M. Tignor and H.L. Miller (eds.)]. Cambridge University Press, Cambridge, United Kingdom and New York, NY, USA.

IPCC, 2000. Special report on emissions scenarios. A Special Report of Working Group III of the Intergovernmental Panel on Climate Change. IPCC. (Available online at http://www.ipcc.ch/pdf/special-reports/spm/sres-en.pdf).

NARCCAP, 2008. The A2 Emissions Scenario. North American Regional Climate Change Assessment Program, National Center for Atmospheric Research (NCAR). Boulder, Colorado, USA. (http://www.narccap.ucar.edu/about/emissions.html).

Robert, C., 2007. Downscaling: An imperative to assess climate change at regional to local scales. In: Workshop on Adaptation of Climate Scenarios to Arctic Climate Impact Assessments, Oslo, Norway: 14-16 May 2007.

Spak, S., Holloway, T., Lynn, B., and Goldberg, R., 2007. A comparison of statistical and dynamical downscaling for surface temperature in North America. J. Geophys. Res., 112, D08101.

Sun, L., 2009. Use of regional climate models for seasonal prediction lessons for climate change application. Workshop on Evaluating and Improving Regional Climate Projections. International Research Institute for Climate and Society, Toulouse, France: 11-13 February.

United Republic of Tanzania (URT)., 2001. Agricultural Sector Development Strategy (ASDS). Ministry of Agriculture, Dar-es Salaam, Tanzania.

Watson, R.T., Zinyowera, M.C. and Moss., R.H., 1998. The Regional Impacts of Climate Change: An Assessment of Vulnerability. Cambridge University Press.

Wilby, R.L., Charles, S.P., Zorita, E., Timbal, B., Whetton, P. and Mearns, L.O., 2004. Guidelines for use of climate scenarios developed from statistical downscaling methods. Available from the DDC of IPCC TGCIA, 27 pp.

World Bank., 2002. World Bank Development Indicators. On CD Rom. World Bank, Washington, DC.

Tables:

Table 1. Description of the four GCM models used in the study.

Acronym	Model	Source
IPSL	Ipsl_cm4	Institut Pierre Simon Laplace
ECHAM	mpi_echam5	Max Planck Institut für Meteorologie
CGCM	cccma_cgcm3_1	Canadian Centre for Climate Modelling and Analysis
CNRM	cnrm_cm3	aMétéo-France/Centre National de Recherches Météorologiques model

Table 2. Comparison between observed and NCEP re-analysis rainfall for the 1979-2004 during March-April-May (MAM) season.

	Mean		Std*		Maximum		Minimum	
Observations	Obs**	NCEP	Obs	NCEP	Obs	NCEP	Obs	NCEP
Seasonal rainfall (mm)	243.3	193.8	89.4	89.9	442.6	476.2	118.0 ***a***	28.04 ***b***
2 mm rainfall events	19.1	17.1	4.1	4.9	27.0	29.0	10	4
10 mm rainfall events	7.2	5.7	7.2	5.6	15.0	13.0	3	0
Maximum dry spell (days)	21.3	20.5	6.4	4.4	43.0	36	12	14
Seasonal start dates (DOY)	69.6	71.5	11.8	13.2	88	86	52	52
Seasonal end dates (DOY)	146.6	149.2	19.1	10.4	180	167	115	127
Seasonal length (days)	77.0	77.7	18.7	15.5	108	106	41	42

*Std – standard deviation

Obs – observed; ***a* and ***b*** = significant at P<0.01 and P<0.05, respectively; DOY = day of the year

Table 3. Comparison between observed and NCEP re-analysis rainfall for the 1979-2004 during October-November-December (OND) season.

	Mean		Std		Maximum		Minimum	
Observations	Obs**	NCEP	Obs	NCEP	Obs	NCEP	Obs	NCEP
Seasonal rainfall (mm)	162.0	128.2	121.6	64.6	596.4 ***a***	292.7 ***b***	17.5 ***a***	43.66 ***b***
2 mm rainfall events	14.0	12.5	8.4	5.6	38	28	2 *a*	6 *b*
10 mm rainfall events	5.3	4.1	4.4	2.8	20***a***	12***b***	0	0
Maximum dry spell (days)	24.4	25.5	7.9	5.3	43	36	14	16
Seasonal start dates (DOY)	302.7	299.8	18.7	21.3	331	333	279	268
Seasonal end dates (DOY)	413.0	423.5	43.2	58.2	504	543	374	374
Seasonal length (days)	109.8	122.5	43.2	59.7	198	262	46	55

*Std – standard deviation

Obs – observed; ***a* and ***b*** = significant at P<0.01 and P<0.05, respectively; DOY = day of the year

Table 4. Comparison between NCEP reanalysis and GCM models rainfall for the 1979-2000 during March-April-May (MAM) season.

Parameters	NCEP reanalysis	GCM Models			
		CGCM	CNRM	IPSL	ECHAM
Seasonal rainfall (mm)	208.1	197.2	182.3	207.1	168.2
2 mm rainfall events	17.9	18.0	16.5	18.7	15.7
10 mm rainfall events	6.2	6.4	6.2	6.5	5.3
Maximum dry spell (days)	20.0	21.0	21.9	19.0	21.0
Seasonal start dates (DOY)	71.5	69.0	76.5	74.8	64.1
Seasonal end dates (DOY)	149.1	158.0	160.9	175.8 ***a***	146.5
Seasonal length (days)	77.6	89.1	84.4	101.0 ***b***	82.4

a and ***b*** = significant at P<0.01 and P<0.05, respectively; DOY = day of the year

Table 5. Comparison between NCEP reanalysis and GCM models rainfall for the 1979-2000 during October-November-December (OND) season.

Parameters	NCEP reanalysis	GCM Models			
		CGCM	CNRM	IPSL	ECHAM
Seasonal rainfall (mm)	132.3	135.2	201.0 ***a***	144.5	164.6
2 mm rainfall events	13.0	13.9	17.0 ***b***	13.2	15.2
10 mm rainfall events	4.2	4.4	7.0 ***b***	4.9	5.5
Maximum dry spell (days)	25.0	27.2	21.1 ***b***	24.6	21.9
Seasonal start dates (DOY)	300.7	306.3	295.4	311.9	298.2
Seasonal end dates (DOY)	428.4	387.4	396.3	381.9	442.7
Seasonal length (days)	127.7	118.6	128.3	98.6	175.4

a and ***b*** = significant at P<0.01 and P<0.05, respectively; DOY = day of the year.

Table 6. Preferential choices of GCM models that their averages provide better prediction of a specific rainfall parameter, and which correspond well with values obtained using NCEP reanalysis.

Parameter	MAM models	Avg values	OND models	Avg values
Seasonal rainfall (mm)	CGCM, IPSL	202.2	CGCM, IPSL	139.9
2 mm rainfall events	CGCM, IPSL, CNRM,ECHAM	17.2	CGCM, IPSL	13.6
10 mm rainfall events	CGCM, IPSL, CNRM	6.4	CGCM, IPSL	4.7
Maximum dry spell (days)	CGCM, IPSL, CNRM, ECHAM	20.7	CGCM, IPSL	25.9
Seasonal start dates (DOY)	CGCM, IPSL, CNRM, ECHAM	71.1	CGCM,ECHAM,CNRM	300.0
Seasonal end dates (DOY)	ECHAM	146.5	ECHAM	442.7
Seasonal length (days)	ECHAM, CNRM	83.4	CNRM	128.3

Avg – average; DOY = day of the year

Table 7. Projected rainfall changes of GCM models' downscaled data during March-April-May for the 2046 – 2065 period.

	Rainfall parameters*						
GCM models	>2mm rainfalls	>10mm rainfalls	Seasonal rainfall (mm)	Max. dry spell (days)	Start dates (days)	End dates (days)	Seasonal length (days)
CGCM	3.5 ***b***	2.7 ***ab***	69.4 ***ab***	-2.3	0.1	11.1	11.1
CNRM	3.6 ***b***	1.8	49.6 ***b***	-2.8	-4.3	-0.5	3.9
IPSL	2.8 ***b***	2.6 ***ab***	61.0 ***ab***	-0.7	-2.8	2.4	5.1
ECHAM	3.3	1.4	42.4	-0.9	-3.2	8.4	11.5
Average	**3.3**	**2.1**	**55.6**	**-1.7**	**-2.6**	**5.4**	**7.9**

* Negative value indicates a decrease and positive value an increase in the observed parameter; ***a*** and ***b*** = significant at P<0.01 and P<0.05, respectively.

Table 8. Projected rainfall changes of GCM models' downscaled data during October-November-December for the 2046 –2065 period.

	Rainfall parameters*						
GCM models	>2mm rainfalls	>10mm rainfalls	Seasonal rainfall (mm)	Max. dry spell (days)	Start dates (days)	End dates (days)	Seasonal length (days)
CGCM	2.3	1.1	32.8	-2.3	-1.7	56.9 ***ab***	59.5 ***ab***
CNRM	4.2 ***b***	2.6 ***b***	57.2	-2.9	-8.5	10.8	20.7
IPSL	2.1	1.2	30.6	-0.9	-0.4	40.1	39.6
ECHAM	3.6 ***b***	2.7 ***ab***	49.6 ***b***	-2.1	-9.2	33.8	42
Average	**3.0**	**1.9**	**42.5**	**-2.1**	**-4.9**	**35.4**	**40.4**

* Negative value indicates a decrease and positive value an increase in the observed parameter; ***a*** and ***b*** = significant at P<0.01 and P<0.05, respectively.

Table 9. Projection of precipitation changes by different GCM models during the 2081 – 2100 (*Future-B*) periods for March-April-May season.

	Rainfall parameters*						
GCM models	>2mm rainfalls	>10mm rainfalls	Seasonal rainfall (mm)	Max. dry spell (days)	Start dates (days)	End dates (days)	Seasonal length (days)
CGCM	6.2 ***ab***	5.6 ***ab***	153 ***ab***	-3.6 ***b***	-2.7	13.8	16.4
CNRM	5.7 ***ab***	4.1 ***ab***	101.6 ***ab***	-3.0	-8.0	10.0	18.0
IPSL	4.9 ***ab***	4.5 ***ab***	104.2 ***ab***	-1.6	-5.7	4.2	9.8
ECHAM	6.2 ***ab***	3.0 ***ab***	93.8 ***ab***	-4.4 ***b***	-7.4 ***b***	14.3	21.7 ***b***
Average	**5.7**	**4.3**	**113.1**	**-3.1**	**-5.9**	**10.6**	**16.5**

* Negative value indicates a decrease and positive value an increase in the observed parameter; ***a*** and ***b*** = significant at P<0.01 and P<0.05, respectively.

Table 10. Projection of precipitation changes by different GCM models during the 2081 – 2100 (*Future-B*) periods for October-November-December season.

GCM models	Rainfall parameters*						
	>2mm rainfalls	>10mm rainfalls	Seasonal rainfall (mm)	Max. dry spell (days)	Start dates (days)	End dates (days)	Seasonal length (days)
CGCM	3.9 ***ab***	1.6 ***b***	49.7 ***ab***	-3.4	-6.1	60.1 ***ab***	65.1 ***ab***
CNRM	3.7	2.1 ***b***	61.2 ***b***	-2.8	-4.7	74.2 ***ab***	80.3 ***ab***
IPSL	3.0 ***b***	1.8 ***b***	49.6 ***ab***	-3.0	-9.1	59.4 ***b***	67.5 ***ab***
ECHAM	4.7 ***ab***	3.2 ***ab***	71.6 ***ab***	-2.6	-0.7	35.5	36.0
Average	**3.8**	**2.2**	**58.0**	**-2.9**	**-5.1**	**57.3**	**62.2**

* Negative value indicates a decrease and positive value an increase in the observed parameter; ***a*** and ***b*** = significant at P<0.01 and P<0.05, respectively.

Table 11. Projection of annual maximum temperature changes (^{o}C) by different GCM models in 2046 to 2065 and 2081 to 2100.

Periods	Temperature variables	CGCM	CNRM	IPSL	ECHAM	average
Control period (1961-2000)	Mean temperature	29.1	29.1	29.1	29.1	29.0
	Standard deviation	3.0	2.9	2.9	2.8	2.9
	Maximum temperature	38.7	38.7	38.7	38.7	38.4
	Min temperature	19.4	19.9	19.4	19.9	19.6
Future-A (2046-2065)	Mean temperature	31.1	31.2	31.4	30.8	31.0
	Standard deviation	3.0	2.9	3.0	2.8	2.9
	Maximum temperature	39.4	41.1	41.3	40.6	40.6
	Min temperature	22.1	22.1	21.6	22.0	21.8
Future-B (2081-2100)	Mean temperature	32.6	33.5	33.7	33.2	33.1
	Standard deviation	3.0	3.1	3.1	2.8	3.0
	Maximum temperature	40.9	42.6	42.9	41.5	41.7
	Min temperature	22.9	24.2	24.3	23.3	23.3
Change	***Future-A* (2046-2065)**	**2.0**	**2.2**	**2.3**	**1.7**	**2.0**
	***Future-B* (2081-2100)**	**3.5**	**4.4**	**4.5**	**4.1**	**4.0**

Table 12. Projection of annual minimum temperature (^{o}C) changes by different GCM models in 2046 to 2065 and 2081 to 2100.

Periods	Temperature variables	CGCM	CNRM	IPSL	ECHAM	average
Control period (1961-2000)	Mean temperature	17.8	17.8	17.8	17.8	17.8
	Standard deviation	2.0	2.0	2.0	2.0	1.9
	Maximum temperature	22.7	22.2	22.7	22.7	22.4
	Min temperature	10.0	10.0	10.6	10.6	10.4
Future-A (2046-2065)	Mean temperature	20.0	20.2	20.3	19.7	19.9
	Standard deviation	2.0	2.0	2.1	1.9	1.9
	Maximum temperature	24.5	24.7	24.8	24.2	24.3
	Min temperature	12.2	12.0	12.8	12.7	12.4
Future-B (2081-2100)	Mean temperature	21.6	22.5	22.7	22.3	22.0
	Standard deviation	2.0	2.1	2.1	2.0	2.0
	Maximum temperature	26.8	28.2	27.7	27.0	27.2
	Min temperature	13.1	15.1	14.4	15.3	14.3
Change	***Future-A* (2046-2065)**	**2.2**	**2.3**	**2.4**	**2.0**	**2.1**

***Future-B* (2081-2100)**	**3.9**	**4.7**	**4.9**	**4.5**	**4.3**

Figures:

Figure 1. **Map of Tanzania showing Same district area.**
(*Source: http://dspace.dial.pipex.com/suttonlink/350map.html*).

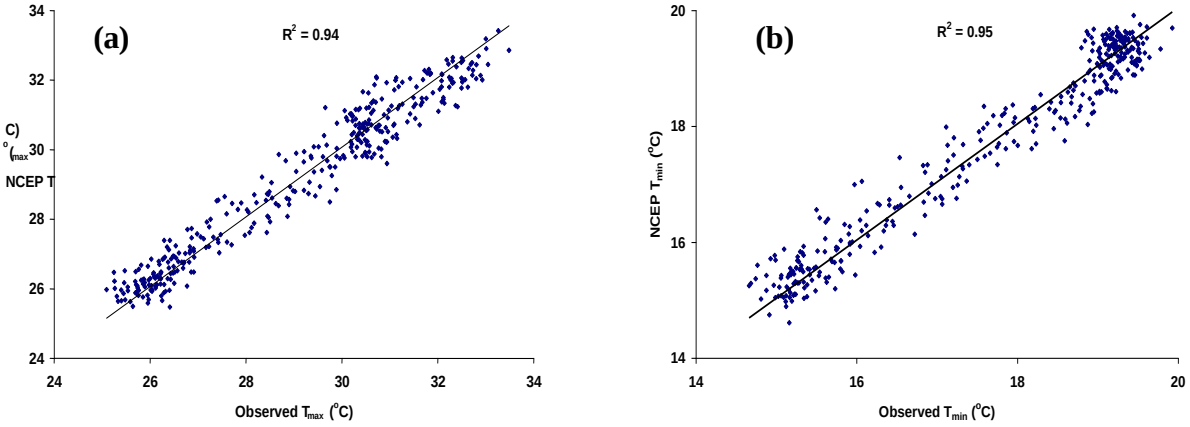

Figure 2. **Comparison of the observed and predicted (a) maximum and (b) minimum temperatures based on SOM technique and NCEP reanalysis for Same region.**

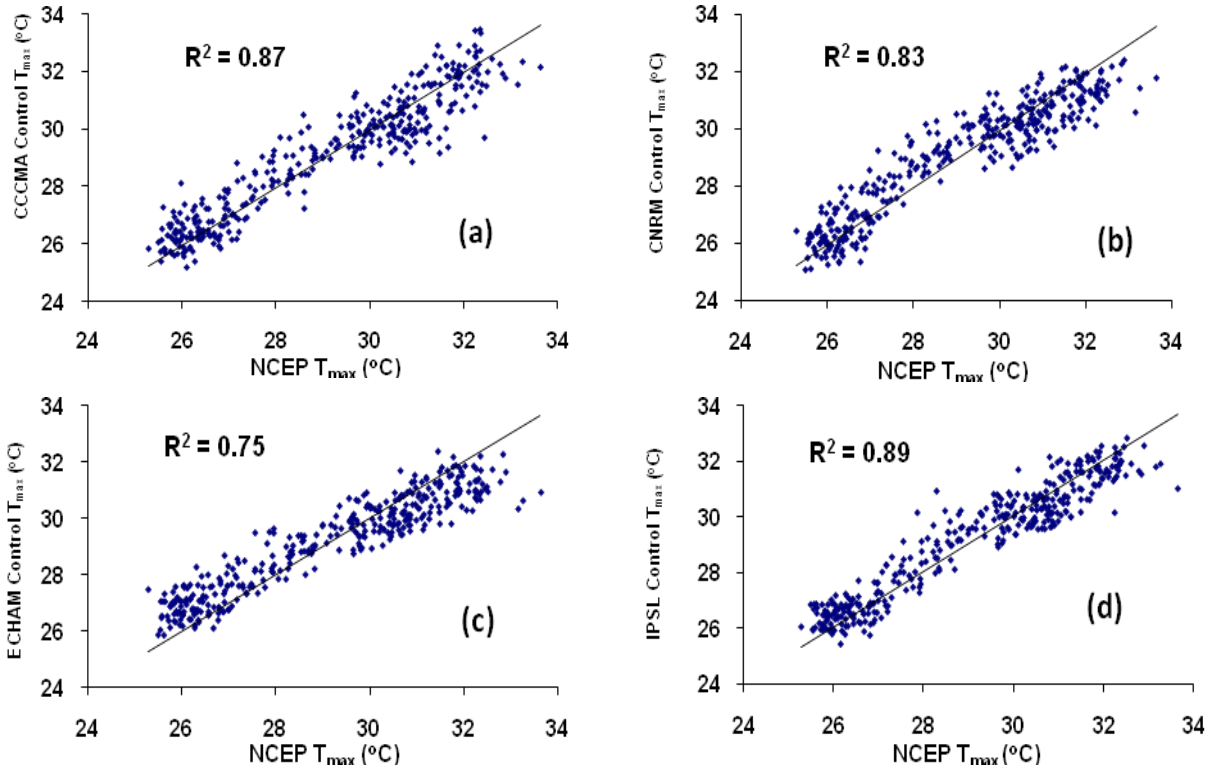

Figure 3. Comparison between NCEP reanalysis and GCM models maximum temperature predictions for the period between 1961 and 2000 for a) CCCMA, b) CNRM, c) ECHAM, and d) IPSL controls.

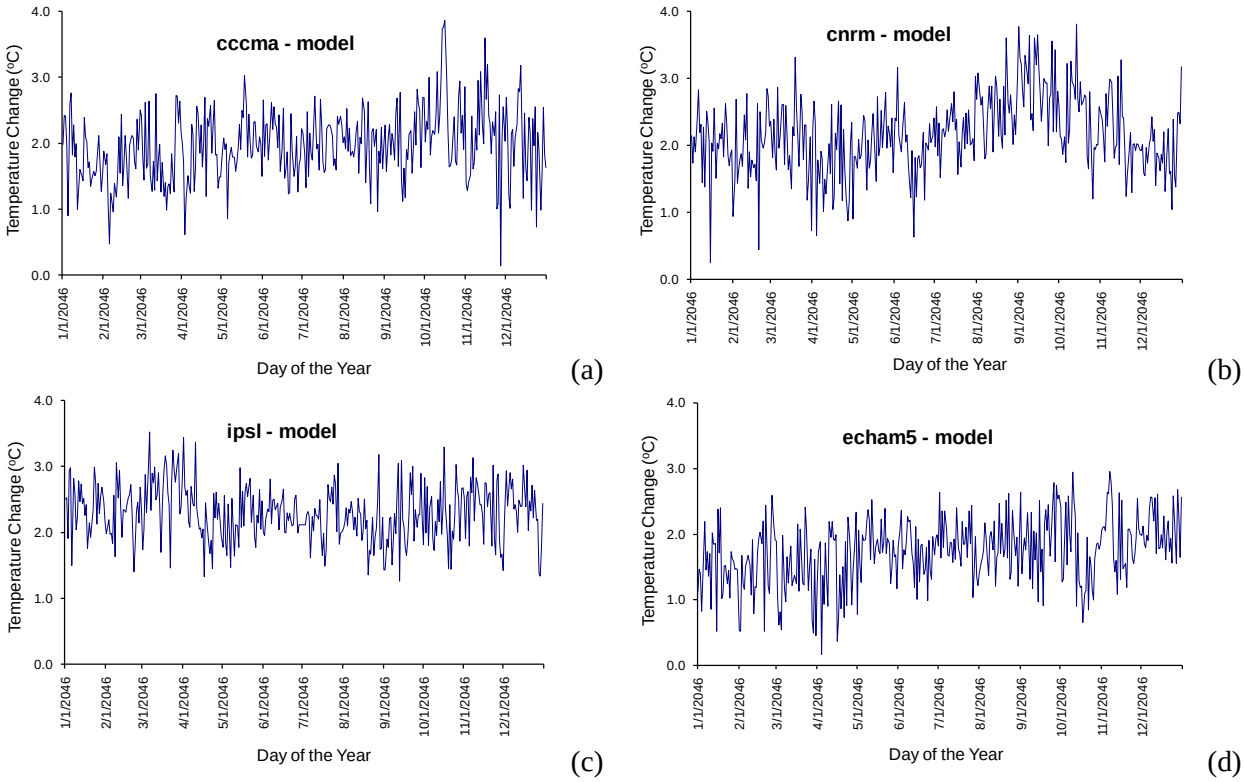

Figure 4. Projection of annual temporal maximum temperature changes by different GCM models for the 2046 to 2065 period.